A NUMERICAL AND EXPERIMENTAL ANALYSIS OF HEAT TRANSFER IN A WAVY FIN-AND-TUBE HEAT EXCHANGER

Igor Wolf [1)], Bernard Franković [1)], Ivan Viličić [1)],
Romuald Jurkowski [2)], André Bailly [2)]
[1)] Faculty of Engineering University of Rijeka, Vukovarska 58,
HR-51 000 Rijeka, Croatia
E-mail: igorw@riteh.hr, bernardf@riteh.hr, ivilicic@riteh.hr
[2)] Research and Development Center, CIAT, Avenue J. Falconnier,
F-01350 Culoz, France
E-mail: r.jurkowski@ciat.fr, a.bailly@ciat.fr

Abstract: *A physical process of heat transfer on the air-side of a wavy fin-and-tube heat exchanger has been analysed numerically and experimentally in this paper. The heat exchanger studied has three rows of circular tubes in a staggered arrangement. A three-dimensional steady-state fluid flow and heat transfer mathematical model has been solved using CFD software based on control volume numerical method. The numerical results have been compared to experimental measurements and Wang's empirical correlations. Compatibility between the results has been found.*

Key words: Heat exchanger, finned tube, numerical analysis, experiment

1. INTRODUCTION

The contribution of air-conditioning systems in energy consumption has been growing very fast in recent years. The increased usage of air conditioners has resulted in an increase in the amount of electricity consumption, especially in summer periods, which has caused instability in electricity supply, expensive infrastructure requirement of a state's power plant and electrical distribution system, as well as a substantial environmental impact. That fact has challenged the air conditioner manufacturers to improve energy efficiency of their products and reduce the electricity consumption.

The performance of an air-conditioning unit is closely dependent on the performances of its constituent devices - heat exchangers, compressors and fans. The most significant opportunity for electrical power use reduction of air conditioners is in technology improvement of the heat exchangers. To be able to achieve the goal - improvement of energy efficiency, reduction of energy consumption and impact on the environment - highly extensive knowledge of the physical phenomena involved is required.

The aim led manufacturers at first to the use of experimental results. This method was followed by the development of analytical tools that enabled the optimal use and extrapolation of experimental results. But, the best insight into the nature of a physical process can be given by a numerical approach. Initially reserved for academic research centres, improvement of the ergonomics of numerical products and the intensive progress in the IT sector raised the interest of the manufacturers for numerical analyses. They realized that this method offers significant reduction in development costs and time.

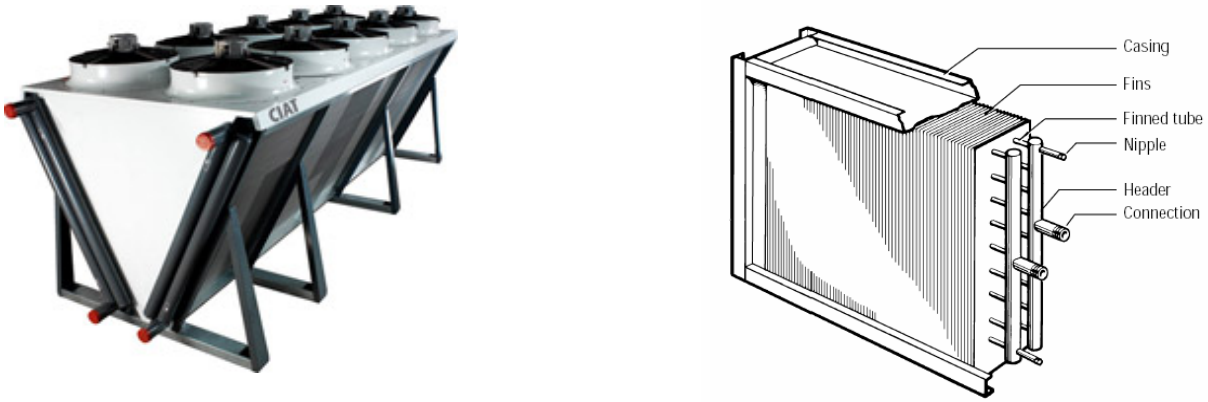

Figure 1. Some examples of fin-and-tube heat exchangers

The present work shows some results of a numerical analysis carried out in order to investigate heat transfer on the air-side of a fin-and-tube heat exchanger. Fin-and-tube heat exchangers (Figure 1) are widely used in air-conditioning systems, as well as in any other application requiring heat exchange between liquids and gases. They consist of mechanically or hydraulically expanded tubes in a block of parallel continuous fins. Taking into consideration air-conditioning systems, water or a refrigerant (R134a, R410a, R407c etc.) is forced to flow through the tubes, while air is directed across the tubes. The dominant thermal resistance is generally on the air side (more than 85% of the total resistance). To effectively improve the performances of the heat exchangers, enhanced surface geometries are employed (Figure 2). There is, however, a continual trade-off between increasing the heat transfer coefficient of the heat exchanger and increasing the frictional pressure drop.
The analysis and modelling of a fin-and-tube heat exchanger is far from trivial. The air side flow around the tube bundle and through the fin gaps is a very complex process. Hence, most of the work published is based on experimentation. Some of the works devoted to the subject can be found in [1–12].

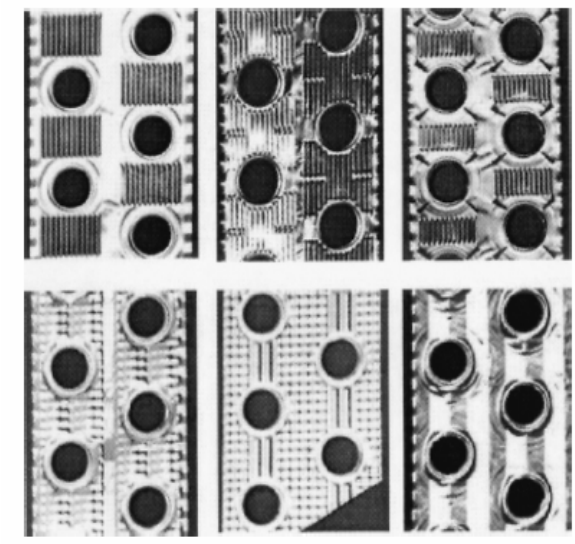

Figure 2. Examples of fin patterns

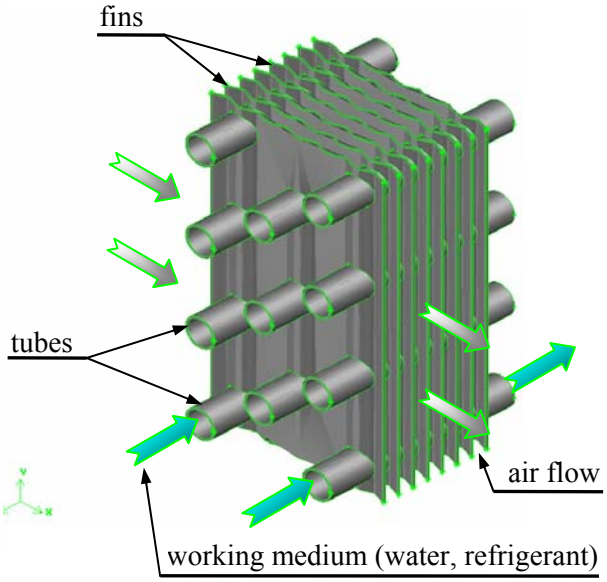

Figure 3. Wavy fin-and-tube heat exchanger

In this paper, some results of a three-dimensional numerical analysis of heat transfer on the air-side of a wavy fin-and-tube heat exchanger are presented. The heat exchanger studied has three rows of circular tubes in a staggered arrangement (Figure 3). The wavy fin pattern has been chosen because of its popularity owing to better air flow mixing and higher heat transfer coefficients compared to plain fins, without causing a considerable increase in pressure drop. Investigations are carried out for different values of the inlet frontal velocity ranging from 1 to 4 m/s. The numerical results have been validated with experimental data obtained by experimental investigations performed in the Research and Development Centre of the *Compagnie Industrielle d'Applications Thermiques* (CIAT), Culoz, France.

2. MATHEMATICAL MODEL

Figure 4 shows the three-dimensional computational domain used in this study. The upstream boundary of the domain is located one fin length before the heat exchanger while the downstream boundary is set at two fin lengths after it. The air flow is assumed incompressible with constant properties, steady and turbulent. The Reynolds-averaged equations can be expressed as follows:

Continuity
$$\operatorname{div}\vec{w} = 0 \tag{1}$$

Momentum x...
$$\operatorname{div}\left(\rho u \vec{w}\right) = -\frac{\partial p}{\partial x} + \operatorname{div}\left(\mu \operatorname{grad} u\right) \tag{2}$$

y...
$$\operatorname{div}\left(\rho v \vec{w}\right) = -\frac{\partial p}{\partial y} + \operatorname{div}\left(\mu \operatorname{grad} v\right) \tag{3}$$

z...
$$\operatorname{div}\left(\rho w \vec{w}\right) = -\frac{\partial p}{\partial z} + \operatorname{div}\left(\mu \operatorname{grad} w\right) \tag{4}$$

Energy
$$\rho c_p \operatorname{div}\left(T \vec{w}\right) = \operatorname{div}\left(\lambda \operatorname{grad} T\right) \tag{5}$$

The standard k-ε turbulent model has been used in the present work. This model uses the following transport equations:

$$\frac{\partial(\rho k)}{\partial t} + \operatorname{div}\left(\rho k \overline{\vec{w}}\right) = \operatorname{div}\left[\frac{\mu_t}{\sigma_k} \operatorname{grad} k\right] + 2\,\mu_t\,\overline{e}_{ij}\,\overline{e}_{ij} - \rho\,\varepsilon \tag{6}$$

$$\frac{\partial(\rho \varepsilon)}{\partial t} + \operatorname{div}\left(\rho \varepsilon \overline{\vec{w}}\right) = \operatorname{div}\left[\frac{\mu_t}{\sigma_\varepsilon} \operatorname{grad} \varepsilon\right] + C_{1\varepsilon}\frac{\varepsilon}{k} 2\,\mu_t\,\overline{e}_{ij}\,\overline{e}_{ij} - C_{2\varepsilon}\,\rho\frac{\varepsilon^2}{k} \tag{7}$$

The fluid region comprises entrance, outlet and bundle zone, as shown in Figure 4. At the upstream boundary, the dry air entering the computational domain is assumed to have uniform velocity (1 - 4 m/s), temperature (297 K) and turbulent intensity (3%). At the end of the computational domain, the streamwise gradient for all variables is set equal to zero. The solid region includes two fins with half a fin thickness and tubes. Heat conduction in the fins is taken into consideration. The tube surface temperature is constant (283 K). At all the solid surfaces no-slip condition for the velocity is specified. Periodic boundary condition is set for the boundaries of the computational domain parallel to the fins. A symmetrical boundary condition is applied to the boundaries on each side of the domain in the y direction, i.e. normal gradients are equal to zero. All the air and material physical properties are constant.

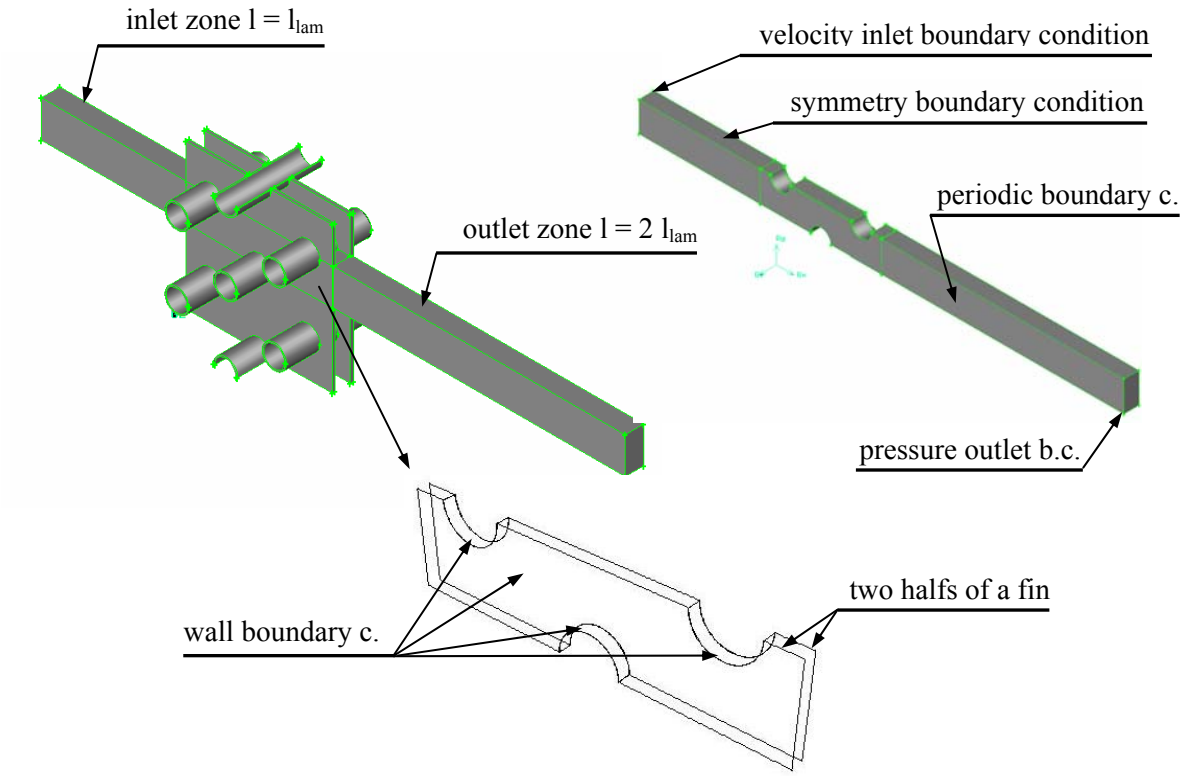

Figure 4. Computational domain

3. NUMERICAL ANALYSIS

The set of governing differential equations (1)-(7) has been solved by a commercially available CFD software *Fluent* based on the finite volume method [13, 14]. The computational mesh consists of around 500 000 cells (Figure 5). A second order upwind scheme has been used to discretize the convection-diffusion terms. The SIMPLE algorithm has been used to solve the pressure and velocity fields. The solution is assumed to be converged when the residuals are less than 10^{-3} for the continuity and momentum equations and less than 10^{-8} for the energy equation.
The detailed geometry of the tested heat exchanger is given in Table 1.

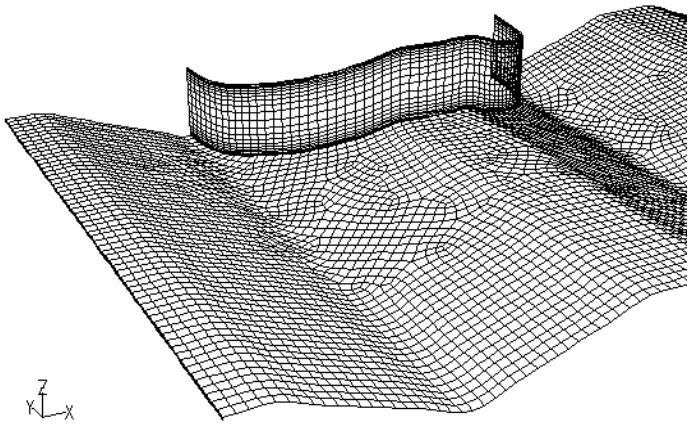

Figure 5. A part of the computational mesh

Table 1. Geometric specification of analyzed heat exchanger

Outside tube diameter	7,94 mm
Longitudinal tube pitch	16,0 mm
Transversal tube pitch	24,0 mm
Wave height	1,15 mm
Wave angle	19,2º
Proj. fin pattern length	3,30 mm
Fin length	48,0 mm
Fin thickness	0,10 mm
Fin pitch	1,60 mm
Number of rows	3

4. DATA REDUCTION

The following calculations are employed to determine the air-side heat transfer characteristics from the data obtained by the numerical analysis. The air-side heat transfer rate was calculated according to Eq. (8):

$$\dot{Q} = \dot{H}_{\mathrm{izl}} - \dot{H}_{\mathrm{ul}} . \tag{8}$$

Enthalpy flow rates at the inlet $\dot{H}_{\mathrm{ul}}$ and outlet $\dot{H}_{\mathrm{izl}}$ of the computational domain has been determined with the aid of *Fluent*. Then, the average air-side heat transfer coefficient can be calculated from Eq. (9):

$$\alpha_{\mathrm{zr}} = \frac{\dot{Q}}{\eta_{\mathrm{uk}}\ A_{\mathrm{zr,uk}}\ \Delta T_{\log}}, \tag{9}$$

where $A_{\mathrm{zr,uk}}$ is the overall surface of the heat exchange on the air-side, while $\Delta T_{\log}$ is the logarithmic mean temperature difference calculated as:

$$\Delta T_{\log} = \frac{T_{\mathrm{zr,ul}} - T_{zr,\mathrm{izl}}}{\ln \dfrac{T_{\mathrm{zr,ul}} - T_{\mathrm{st}}}{T_{\mathrm{izr,zl}} - T_{\mathrm{st}}}} . \tag{10}$$

T_{st} is the tube surface temperature given as a wall boundary condition.
The overall surface effectiveness (η_{uk}), which is defined as the ratio of the effective heat transfer area to the total heat transfer area, can be expressed in terms of fin efficiency (η_{lam}), fin surface area (A_{lam}) and total surface area ($A_{\mathrm{lam}} + A_{\mathrm{baza}}$) as follows:

$$\eta_{\mathrm{uk}} = 1 - \frac{A_{\mathrm{lam}}}{A_{\mathrm{lam}} + A_{\mathrm{baza}}} \cdot \left(1 - \eta_{\mathrm{lam}}\right). \tag{11}$$

The fin efficiency (η_{lam}) has to be calculated iteratively from Eqs. (12) - (13) and Eq (9):

$$\eta_{\mathrm{lam}} = \frac{\tanh\left(m r_{\mathrm{u}} \phi\right)}{m r_{\mathrm{u}} \phi}, \quad m = \sqrt{\frac{2\,\alpha_{\mathrm{zr}}}{\lambda_{\mathrm{lam}} \delta_{\mathrm{lam}}}}, \quad \phi = \left(\frac{r_{\mathrm{ekv}}}{r_{\mathrm{u}}} - 1\right) \cdot \left(1 + 0{,}35 \ln \frac{r_{\mathrm{ekv}}}{r_{\mathrm{u}}}\right). \tag{12}$$

The analysed heat exchanger is arranged in a staggered layout, so the following equations are applied:

$$\frac{r_{\mathrm{ekv}}}{r_{\mathrm{u}}} = 1{,}27 \frac{X_{\mathrm{M}}}{r_{\mathrm{u}}} \sqrt{\frac{X_{\mathrm{L}}}{X_{\mathrm{M}}} - 0{,}3}, \quad X_{\mathrm{M}} = \frac{P_{\mathrm{t}}}{2}, \quad X_{\mathrm{L}} = \frac{1}{2} \sqrt{\left(\frac{P_{\mathrm{t}}}{2}\right)^2 + P_{\mathrm{l}}^2} . \tag{13}$$

The basic surface characteristics of heat exchangers are usually presented in a dimensionless form as the Colburn j factor and the Fanning friction factor f:

$$j = \mathrm{Nu} / \left(\mathrm{Re}\,\mathrm{Pr}^{\frac{1}{3}}\right), \quad f = \frac{1}{2} \frac{\Delta p}{\rho_{\mathrm{zr}}\ w_{\max}^2} \frac{D_{\mathrm{h}}}{L}, \tag{14}$$

where L is the depth of the heat exchanger, and w_{max} is the maximum air velocity. Hydraulic diameter D_h is equal to:

$$D_h = \frac{4 A_{min} L}{A_{zr,uk}}, \tag{15}$$

where A_{min} is the minimum air free flow area.

5. EXPERIMENTAL APPARATUS

Experimental investigations have been performed at the Research and Development Centre of CIAT company in Culoz, France, in order to evaluate the results of the numerical analysis. A schema of the experimental apparatus is shown in Figure 6.

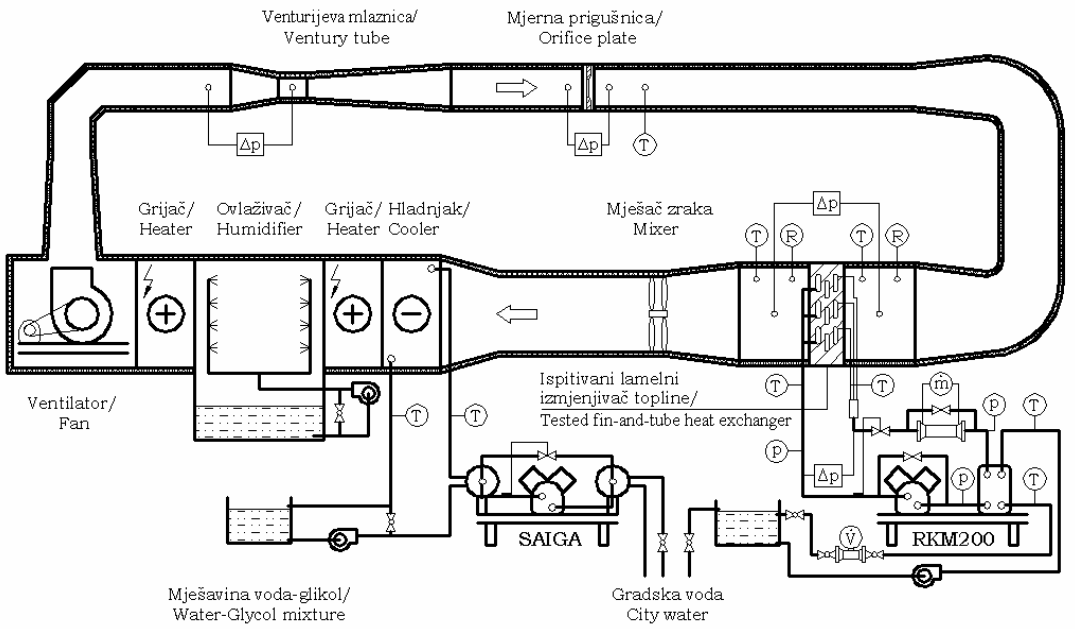

Figure 6. Schema of the experimental apparatus

The experimental assembly, a closed-loop wind tunnel, consists of a centrifugal fan with an inverter, an air velocity measurement section, a test section, an air-conditioning section, a chiller and a heat pump. The frontal air velocity is measured using a Ventury tube or an orifice connected to a differential pressure transducer. The inlet and outlet air temperatures at the test section are measured with nine platinum resistant temperature devices (Pt100) placed upstream and downstream of the tested coil. Two hygrometers are installed for measuring the inlet and outlet air dew points. Constant air properties at the inlet section of the heat exchanger are reached by the use of two electrical heaters and a humidifier. The inlet air temperature and humidity were controlled at approximately 24 °C and 50%, respectively during these tests. The cooler in the air-conditioning section and the chiller (Figure 6, SAIGA) were not used.

The coil in the test section is connected to the heat pump (Figure 6, RKM200). The working fluid (R410a) passes through the tubes of the coil and evaporates, while the air becomes cold and dehumidified. Refrigerant temperatures at the inlet and outlet sections of the coil are

measured by 18 K-type thermocouples. In this case, the evaporation temperature was kept constant at 5 °C. The coil heat transfer rate was computed from the measured mass flow rate and temperature change on the refrigerant-side, and, independently, from the mass flow rate and enthalpy change on the air-side. The difference between the air-side and the refrigerant-side heat transfer values was less than 5% for most of the tests.
All the data signals were collected and converted by a data acquisition system, which transmits the signals to the host computer for further operation.

6. RESULTS AND DISCUSSION

The modelling of heat and mass transfer, which occurs during condensation of the water vapour present in the air in the cooling mode, is a complex problem. To simplify the numerical model, the process of the water vapour condensation is neglected in the present study. For that reason, some discrepancies are expected between the numerical and experimental data. Figures 7 and 8 show a comparison of the results obtained. In Figure 7, the numerical and experimental average Nusselt numbers are plotted versus the frontal air velocity. The frontal air velocities correspond to Reynolds numbers in the range of 1 000 to 3 800. The Reynolds numbers are based on the outer tube diameter. It can be seen that the difference between the numerical and experimental values ranges from 4 to 10%. In Figure 8, numerical results for *j* and *f* factors are compared to experimental data and Wang's empirical correlations [16]. Numerical values slightly underestimate (8% max.) *j* factors experimentally obtained in the present study. In comparison with Wang's correlations, the numerical simulation tends to overpredict the *j* factors at low frontal air velocities (max. 17%) and to underpredict them at higher values of the frontal velocity (10%). Numerically calculated friction factors *f* underestimate those calculated from the Wang's correlations max. 23%.

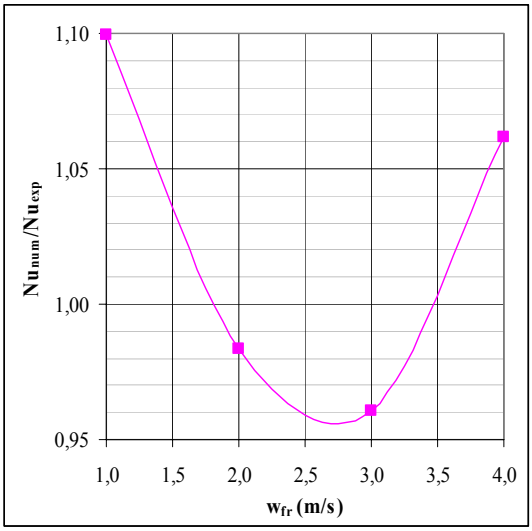

Figure 7. Comparison of average Nusselt numbers

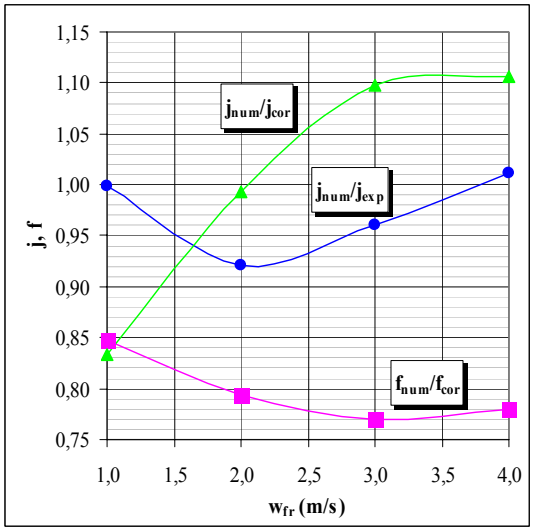

Figure 8. Comparison of *j* and *f* factors

(num – numerical values, exp – experimental values, cor – empirical correlations)

Figures 9 and 10 present the complexity of the flow pattern within a fin-and-tube heat exchanger. The flow accelerates around the tubes and forms a wake region behind the tubes. This causes local variations of the heat transfer coefficients. Figure 9 shows the contours of

velocity magnitudes in the middle plain between the fins for the frontal air velocities of 1 and 4 m/s. The heat transfer coefficient distribution along the fin and around the middle tube for the frontal air velocities of 1 and 4 m/s is shown in Figure 10.

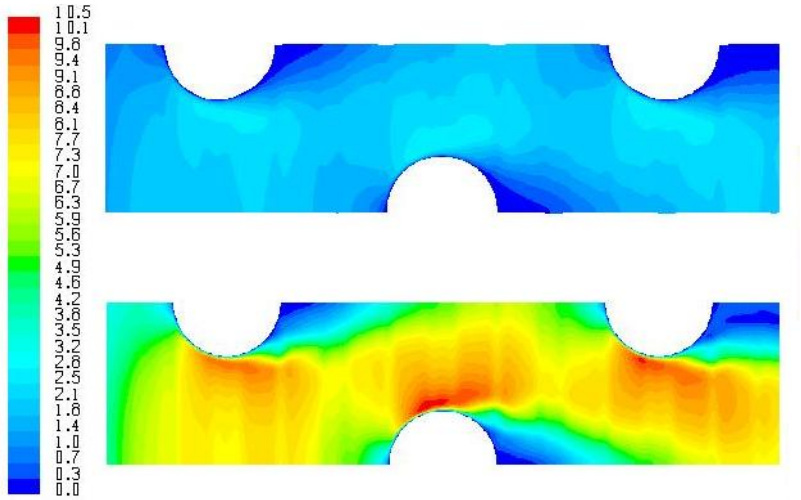

Figure 9. Contours of velocity magnitudes in the middle plane between the fins for the frontal air velocities of 1 and 4 m/s

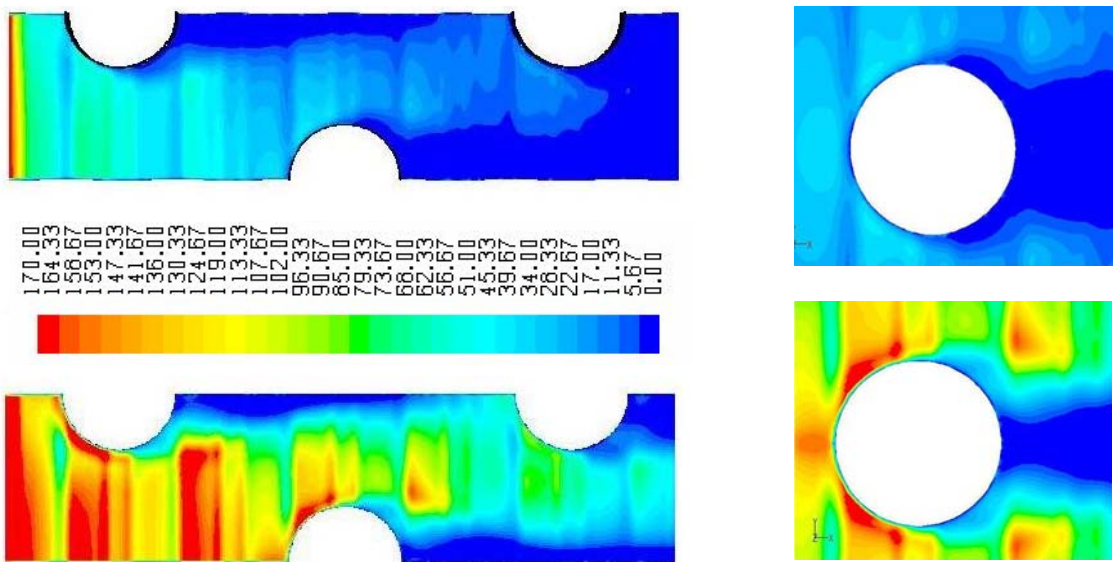

Figure10. Contours of the heat transfer coefficients along the fin and around the middle tube for the frontal air velocities of 1 and 4 m/s, W/m^2K

Near the leading edge of the fin the developing boundary layer produces relatively high heat transfer coefficients, but they fall stringently after it. In front of the tubes, a vortex develops that causes an increase of the heat transfer coefficients. Near the tube centreline the flow separates from the tube which forms a wake region behind the tube. The wake region behind the tube has the smallest values of the heat transfer coefficients.

7. CONCLUSION

A three-dimensional steady-state numerical model was developed to predict the air-side characteristics of a wavy fin-and-tube heat exchanger, widely used as a vital part of air conditioning systems. The heat transfer in fin-and-tube heat exchangers is generally influenced by the strong thermal resistance on the air-side, thus great efforts are being done to effectively increase the air-side convective heat transfer performance. The production of heat pumps and chillers in the last couple of years has been greatly augmented and even small thermodynamic improvements can help to reduce the overall energy consumption and impact on the environment.

The air-side heat transfer and pressure drop characteristics were successfully modelled using the CFD software *Fluent*, based on the control volume numerical method. Experimental investigations were performed to verify the numerical predictions. The numerical results for Colburn *j* and friction *f* factors are compatible with the experimentally obtained values. The numerical model predicts Colburn *j* factors within 8% compared to experimental data. In comparison with Wang's empirical correlations, *j* factors are predicted within 17% and friction factor *f* within 23%. The three-dimensional local flow and thermal fields are well characterized by the numerical analysis.

The developed and presented model demonstrates good heat transfer prediction. It can provide guidelines for design optimization of a fin-and-tube heat exchanger.

8. LIST OF SYMBOLS

a	thermal diffusivity [m^2/s]
A	surface [m^2]
c	specific heat capacity [J/(kgK)]
D	diameter [m]
eij	deformation of a fluid element [N/m2]
f	Fanning friction factor
h	specific enthalpy [J/kg]
j	Colburn factor
k	specific turbulent kinetic energy [J/kg]
L	depth of the heat exchanger [m]
N	number of tube rows
Nu	Nusselt number
p	pressure [Pa]
P_f	fin pitch [m]
P_l	longitudinal tube pitch [m]
Pr	Prandtl number
P_t	transverse tube pitch [m]
$\dot{Q}$	heat flow rate [W]
Re	Reynolds number
r	radius, [m]
T	thermodynamic temperature [K]
u, v, w	velocity component in the x, y and z direction [m/s]
$\vec{w}$	velocity vector
X_M, X_L	geometric parameters
α	heat transfer coefficient [W/(m2K)]

δ thickness [m]
ε turbulent kinetic energy dissipation [m2/s3]
μ dynamic viscosity [Pas]
η_{lam} fin efficiency
η_{uk} surface efficiency
λ thermal conductivity [W/(mK)]
ρ density, [kg/m^3]

Subscripts:

ekv equivalent
fr frontal
h hydraulic
izl inlet
lam fin
min minimum
st wall
t turbulent
u internal
uk overall
ul inlet
v outside
zr air

REFERENCES

[1] Marvillet, C.: *Batteries a ailettes: Analyse des techniques d'intensification*, Note Technique STI/GREThGFD/96/438, 1996.
[2] Jurkowski, R.: *Augmentation du transfert de chaleur à un film ruisselant par adjonction d'une couche métallique poreuse à la paroi*, Thesis, l'Institut national polytechnique de Lorraine, 1986.
[3] Wang, C.C.; Hsieh, Y.C.; Chang, Y.J.; Lin, Y.T.: *Sensible Heat and Friction Characteristics of Plate Fin-and-tube Heat Exchangers Having Plane Fins*, International Journal of Refrigeration, 19(1996)4, 223-230.
[4] Mirth, D.R.; Ramadhyani, S.: *Correlations for Predicting the Air-side Nusselt numbers and Friction Factors in Chilled-water Cooling Coils*, Experimental Heat Transfer, 7(1994), 143-162.
[5] Wang, C.C.; FU, W.L.; Chang, C.T.: *Heat Transfer and Friction Characteristics of Typical Wavy Fin-and-tube Heat Exchangers*, Experimental - Thermal and Fluid Science, 14(1997), 174-186.
[6] Lozza, G.; Merlo, U.: *An Experimental Investigation of Heat Transfer and friction losses of interrupted and Wavy Fins for Fin-and-tube Heat Exchangers*, International Journal of Refrigeration, 24(2001), 409-416.
[7] Wang, C.C.; Lee, W.S.; Sheu, W.J.: *A Comparative Study of Compact Enhanced Fin-and-tube Heat Exchangers*, International Journal of Heat and Mass Transfer, 44(2001), 3565-3573.

[8] Yan, W.M.; Sheen, P.J.: *Heat Transfer and Friction Characteristics of Fin-and-tube Heat Exchangers*, International Journal of Heat and Mass Transfer, 43(2000), 1651-1659.
[9] Ničeno, B., Nobile, E., Franković, B.: *A Numerical Study of Enhanced Heat Transfer Surfaces from Compact Heat Exchanger*, Proceeding of International Congress *Energy and Environment* 1996, Opatija, 255-270.
[10] Jang, J.Y.; Chen, L.K.: *Numerical Analysis of Heat Transfer and Fluid Flow in a Three-dimensional Wavy-fin and Tube Heat Exchanger*, International Journal of Heat and Mass Transfer, 40(1997)16, 3981-3990.
[11] Zhang, M.; Dahl, S.D.: *A Computational Study of Heat Transfer and Friction Characteristics of a Smooth Wavy Fin Heat Exchanger*, Thermo King Corp./Ingersoll-Rand, 1999.
[12] Wolf, I.: *Utjecaj geometrijskih parametara na izmjenu topline i karakteristike strujanja zraka kod lamelnih izmjenjivača topline*, magistarski rad, Tehnički fakultet Sveučilišta u Rijeci, Rijeka, 2004.
[13] Versteeg, H.K.; Malalasekera, W.: *An Introduction to Computational Fluid Dynamics, The finite volume method*, Longman Group Ltd, Essex, Engleska, 1995.
[14] Patankar, S.V.: *Numerical Heat Transfer and Fluid Flow*, Hemisphere, New York, 1998.
[15] Wang, C.C.; Webb, R.; Chi, K.Y.: *Data Reduction for Air-side Performance of Fin-and-tube Heat Exchangers*, Experimental Thermal and Fluid Science, 21(2000), 218-226.
[16] Wang, C.C.; Hwang, Y.M.; Lin, Y.T.: *Empirical Correlations for Heat Transfer and flow friction characteristics of Herringbone Wavy Fin-and-tube Heat Exchangers*, International Journal of Refrigeration 25(2002), 673-680.

NUMERIČKA I EKSPERIMENTALNA ANALIZA IZMJENE TOPLINE NA VALOVITOM LAMELNOM OREBRENJU IZMJENJIVAČA TOPLINE

Sažetak: *U radu je numeričkim i eksperimentalnim putem analiziran fizikalni proces prijelaza topline na izmjenjivaču topline s valovitim lamelnim orebrenjem. Analiziran je izmjenjivač topline s tri reda cijevi u kaskadnom rasporedu. Trodimenzijski matematički model fizikalnih pojava ustaljenoga strujanja zraka i prijelaza topline riješen je numeričkom metodom kontrolnih volumena, uporabom komercijalnoga CFD računalnog programa. Postavljeni numerički model provjeren je usporedbom s eksperimentalnim mjerenjima.Utvrđena je dobra podudarnost rezultata.*

Ključne riječi: izmjenjivač topline**,** orebrene cijevi, numerička analiza, eksperiment